Photo-electrochemical study of TiO₂/Co₃O₄ thin films in polluted

International Journal of Hydrogen Energy 89 (2024) 127–134

Contents lists available at ScienceDirect

International Journal of Hydrogen Energy

journal homepage: www.elsevier.com/locate/he

Photo-electrochemical study of TiO_2/Co_3O_4 thin films in polluted electrolyte: A promising route for coupling hydrogen production with water remediation

Fanny Duquet *, Matthieu Rivallin, Florence Rouessac, Raphaël Costes, Jim Cartier, Christophe Charmette, Stéphanie Roualdès **

Institut Européen des Membranes (IEM), UMR 5635, University of Montpellier, ENSCM, CNRS, 34095, Montpellier, France

ARTICLE INFO

Keywords:
Sol-gel synthesis
TiO_2(-Co_3O_4) thin films
Water splitting
Photo-electrochemical cell
Wastewater treatment
Hydrogen production

ABSTRACT

The use of a photo-electrochemical cell (PEC) to produce hydrogen from wastewater is a promising innovation. In this context, this study investigates the impact of a pollutant on the photo-electrochemical properties of sol-gel synthesized TiO_2 and TiO_2–Co_3O_4 thin films for hydrogen production in a polluted electrolyte. Combining the photocatalytic properties of TiO_2 with the electronic properties of Co_3O_4 offers an effective solution for achieving effective photo-electrochemical properties in polluted environments. Nevertheless, despite the lowest photocatalytic activity, the hybrid thin film TiO_2–Co_3O_4 with the highest Ti/Co ratio (1:0.5) shows the most promising performance with simultaneous 11.4 μmol cm^{-2} h^{-1} H_2 production and 12% acid orange 7 degradation after 3 h irradiation under xenon light without the use of any sacrificial agent. This indicates that the electronic conductivity provided by the presence of Co_3O_4 is a critical property for achieving optimal performance in PEC coupling for hydrogen production and wastewater treatment.

1. Introduction

Since the beginning of the 20th century, global demographic and economic growth has been responsible for the intensification of human activity in all sectors: transport, agriculture and livestock farming, urbanization, technology and energy. This has led to an increase in the extraction, processing and use of natural resources, resulting in their depletion and the pollution responsible for the global environmental crisis [1–4]. It is therefore important to work towards finding solutions to the current situation before it gets out of hand. The following article will address two of the major contemporary topics: hydrogen production and water remediation.

Hydrogen has the potential to play a key role in the global energy transition, thanks to its versatility in terms of production methods and diverse end uses [5–7] Currently, hydrogen is mainly used in industry for the refining of petroleum, the production of ammonia, methanol, and steel. Hydrogen has a very low bulk density and a very high energy density (143 MJ/kg), which is significantly higher than that of natural gas (55 MJ/kg), gasoline (46 MJ/kg), or coal (24 MJ/kg) [8,9]. This is why, in addition to its traditional role, hydrogen is being considered not only as a promising energy carrier, but also as a fuel or storage medium. Hydrogen can play a key role in decarbonizing the world's dominant zones, with the aim of achieving zero net carbon dioxide emissions by 2050 [10,11]. Nevertheless, despite the considerable increase in low-emission hydrogen production worldwide in 2021 (nearly 20% more than in 2020), it still represents only a small fraction of total production (1 Mt of low-emission production out of 94 Mt of global hydrogen production in 2021), indicating the necessity for further enhancements in green hydrogen production processes [12].

Textile dyes and other industrial colorants represent one of the most significant groups of organic compounds currently posing a significant threat to the environment [13,14]. According to estimates from the World Bank, the textile industry is responsible for generating between 17% and 20% of industrial wastewater, while approximately 200 000 tons of synthetic dyes are lost to the environment annually due to inefficient dyeing processes [15,16]. Due to the large quantity of aromatics present in dyes and their chemical stability, conventional biological treatment methods are ineffective for their degradation, even

* Corresponding author. Department of Physics and Competence Centre for Catalysis, Chalmers University of Technology, SE-412 96, Göteborg, Sweden.
** Corresponding author.
E-mail addresses: fanny.duquet@chalmers.se (F. Duquet), stephanie.roualdes@umontpellier.fr (S. Roualdès).

https://doi.org/10.1016/j.ijhydene.2024.09.287
Received 26 July 2024; Received in revised form 20 September 2024; Accepted 21 September 2024
Available online 26 September 2024

leading to the production of potentially more dangerous by-products [17,18]. This is why it is necessary to investigate another degradation process.

One promising technological innovation which has the potential to be used for the production of green hydrogen and the remediation of water is the photo-electrochemical cell (PEC) [19–21]. It is evident that a technology that integrates these two processes confers a substantial degree of added value.

Photo-electrocatalysis is a combination of electrolysis and photocatalysis: it is based on the immobilization of a photocatalyst on an electrode that will function as a photoanode or photocathode. Photocatalysts are semiconductor materials that, due to their electronic band structure, can generate electron-hole pairs, which can subsequently participate in chemical reactions. In the case of a photoanode, when the energy of the incident radiation is equal to or greater than the energy of the band gap, an electron passes from the valence band to the conduction band of the semiconductor, resulting in the generation of the electron-hole pair. The photogenerated holes migrate to the photoanode/electrolyte interface on the semiconductor surface to participate in the water oxidation reaction, while the photoexcited electrons are transferred to the counter electrode via an external circuit to reduce the water to hydrogen [22,23].

Pollutants present in the medium will be adsorbed on the photoanode surface and can be degraded in diverse ways. One such way is by photogenerated holes, which are powerful oxidants. Another is by free radicals generated during water oxidation, as shown in equations (1)–(4).

$$H_2O + h^+_{VB} \rightarrow HO^{\cdot} + H^+ \quad (1)$$

$$O_2 + e^-_{CB} \rightarrow O_2^{-\cdot} \quad (2)$$

$$H^+ + O_2^- \rightarrow HO_2^{\cdot} \quad (3)$$

$$2HO_2^{\cdot} \rightarrow H_2O_2 + O_2 \quad (4)$$

Two distinct pathways exist for the oxidation of organic pollutants: direct oxidation at the electrode surface and indirect oxidation by strong oxidants generated in situ. In the former, the pollutants are decomposed until they are completely mineralized into carbon dioxide (CO_2) or water [24,25].

Research into the coupling of hydrogen production and water remediation is extensive and involves a wide range of photocatalysts as well as organic and inorganic pollutants [22,26–29].

Titanium dioxide (TiO_2) has been identified as a standard photocatalyst in hydrogen production and organic dyes degradation due to its low toxicity, low cost, chemical stability, excellent photocatalytic performance, and long-term thermodynamic stability compared to other semiconductor materials [30–32]. However, the large band gap energy (3.2 eV) of the TiO_2 catalysts results in limited photocatalytic activity under irradiation energetically higher from UV, such as visible one. One other significant drawback of TiO_2 is the too quick recombination of electron-hole pairs hindering its photocatalytic efficiency [33,34].

Recent studies have demonstrated that in p-type semiconductor metal oxides, such as Co_3O_4, a combination of trivalent and divalent cobalt can facilitate rapid electron transfer in the PEC process [35–39]. This is due to Co_3O_4 high electrical conductivity. In addition, Co_3O_4 is characterized by good light scattering ability, low cost, and stable chemistry, which collectively contribute to the optimal synergy between PC and EC [40].

The study of hybrid materials based on TiO_2 and Co_3O_4 as photoanodes for photo-electrochemical water splitting has been a subject of interest among researchers for several years [41–44]. The hydrogen production with a sacrificial agent (methanol or glycerol) ranges from 20.2 to 1120.0 μmol g^{-1} h^{-1} versus 6.5–41.8 μmol g^{-1} h^{-1} without the agent [42,43,45–47]. And it's has been proved that these hybrid materials are also capable to degrade dye with good efficiency [48–51]. However, no study has coupled hydrogen production with wastewater treatment, which is what our study innovates.

In our case, the photoanodes were synthesized using a sol-gel method, a soft chemistry route, using a bio-based surfactant (GC) with varying titanium-cobalt ratios (1:0, 1:0.25, and 1:0.5), named respectively TiO_2-GC, TiO_2–CoN0.25-GC and TiO_2–CoN0.5-GC. The synthesis process is illustrated in Fig. 1.

The selection of these three photoanodes was based on their photoelectrocatalytic performances in standard electrolyte previously displayed in two articles by our group [52,53]. Their morphological and structural properties was also discussed in these papers (Table 1). The presence of the anatase and rutile phases, which are linked to TiO_2 and of the spinel phase for Co_3O_4, was highlighted. Furthermore, the formation of $Co(OH_2)$ groups on the surface of hybrid photoanodes was demonstrated.

This article represents a further contribution to the research and understanding of these photoanodes. The objective of this study is to examine the potential of the three photoanodes for hydrogen production in the presence of contaminated water, without the use of sacrificial agents. The dye, acid orange 7 (AO7), was selected as the pollutant for this study due to its status as a mono-azo dye, which is frequently employed as a model compound in investigations into the photodegradation of azo dyes by TiO_2-based materials [54–61]. Moreover, approximately 50–70% of the dyes currently available on the market are azo compounds, making AO7 an important pollutant to study [18,62,63].

2. Materials and methods

2.1. Synthesis

The starting materials, titanium (IV) isopropoxide (TTIP, 99.999 % trace metal basis), cobalt nitrate hexahydrate ($Co(NO_3)_2{\bullet}6H_2O$, ≥98%), and nitric acid (HNO_3, ACS reagent 70%), were all purchased from Sigma Aldrich. The polymeric biosurfactant is GBACoco (lot PF345, Surfactgreen, France - named GC), which is bio-based and 100 % renewable. The solutions were prepared via a sol-gel method; 10 mL of TTIP was combined with 16.85 mL of HNO_3 (2 mol L^{-1}). For the cobalt-free solution (TiO_2-GC), 1 g of surfactant was added after the solution had been stabilized. For TiO_2–CoN0.25-GC and TiO_2–CoN0.5-GC samples, cobalt nitrate was introduced in two different molar ratios HNO_3/TTIP/$Co(NO_3)_2{\bullet}6H_2O$ = 1/1/0.25 and 1/1/0.5, respectively. After stabilization, the surfactant was also introduced. Then, the solution (with or without cobalt) was deposited by dip coating (DipMaster 201, Chemat Technology, INC, Northridge, CA, USA) on ITO support (KINTEC, Kowloon, Hong Kong) to get active materials in the form of thin films. The details of the aforementioned procedure have been described in our previous works [52,53].

2.2. Photocatalytic degradation

For photodegradation experiments, materials in the form of powder immerged in a Petri dish containing a solution of AO7 with initial concentration C_0 of 20 ppm were used. The degradation of the compound is observable to the naked eye, as the breakage of the diazo group ($R_2C{=}N_2$) causes the discoloration of the solution. The Beer-Lambert law (Equation (5)) allows for the study of its degradation over time, with A the absorbance, ε the molar absorption coefficient, l the path length and c the concentration of the active compound.

$$A = \varepsilon \times l \times c \quad (5)$$

To approximate a solar spectral distribution, xenon lighting (75 W LOT Quantum Design, wavelength range 250–2700 nm, power density of 3 mW cm^{-2}) was selected due to its ability to emit light within a broad wavelength range, overlapping UV and visible regions. The distance between the xenon irradiation and the AO7 solution was 20 cm. The

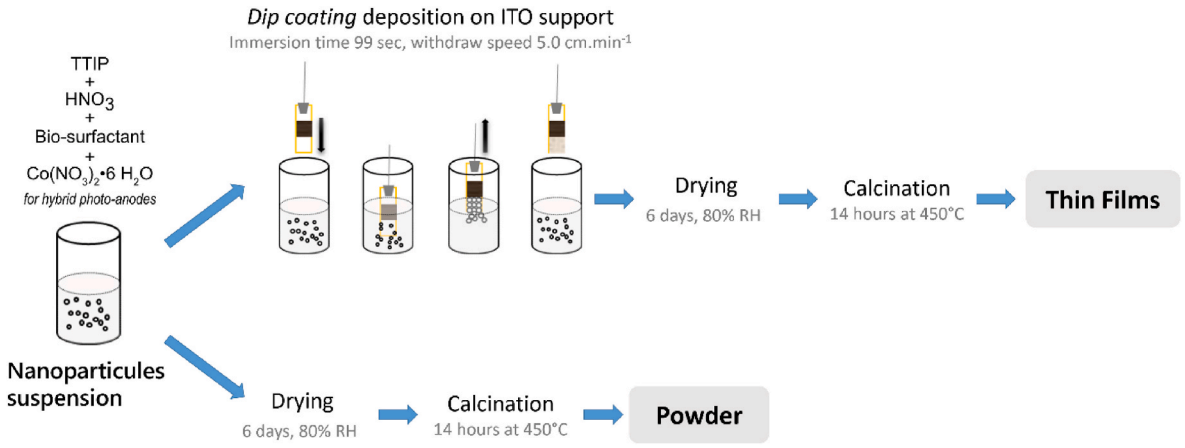

Fig. 1. Synthesis protocol.

Table 1
Highlights of morphological and structural properties for the studied photoanodes from previous articles [52,53].

	TiO_2-GC	TiO_2–CoN0.25-GC	TiO_2–CoN0.5-GC
BET Surface Area ($m^2.g^{-1}$)	101	112	126
Adsorption-Average Pore Width BET (nm)	2.66	4.85	4.27
Anatase/Rutile/Spinel phase (%)	22.4/ 77.6/0.0	47.2/46.7/6.1	37.2/32.9/29.9

photodegradation process was monitored for a period of 7 h. The absorbance was measured on a 1 mL collected solution at the maximum wavelength of AO7, λmax = 486 nm, using a UV–Vis spectrophotometer (JENWAY 7315 Spectrophotometer) at 15-min intervals for the first 90 min, after which the measurement frequency was increased to 30 min. The photodegradation investigation was also performed on materials in the form of thin films in the PEC with or without the electric contribution. In this case, the 1 mL solution collected for UV–Vis spectrophotometry analysis was returned to the cell after analysis.

2.3. Photo-electrochemical characterizations

The photo-electrochemical cell (PEC) equipped with a quartz window was supplied by Pine Research Co USA. Two electrolyte solutions were used, a model one (0.01 mol L^{-1} NaOH – 0.1 mol L^{-1} Na_2SO_4) and a polluted one (0.01 mol L^{-1} NaOH – 0.1 mol L^{-1} Na_2SO_4 – 20 ppm AO7). An Ag/AgCl electrode was used as reference electrode and glass carbon as counter electrode. The photo-anode thin film TiO_2, TiO_2–CoN0.25 or TiO_2–CoN0.5 was the working electrode. Cyclic voltammetry experiments were monitored on a Solartron SI 1287 and curves were measured from 0.0 V/RHE to 2.0 V/RHE at a scan rate of 50 mV s^{-1} under xenon light. Impedance spectroscopy experiments were done on a Solartron SI 1260 and the Nyquist plot was measured in the dark at the onset potential over the frequency range from 0.1 Hz to 10^6 Hz using an AC voltage of 10 mV amplitude. No stirring of the electrolyte solutions was performed due to risk of disruption of the electrochemical signals.

2.4. Hydrogen production

The hydrogen production was measured with the same set-up and solutions that the ones used for photo-electrochemical characterizations, by performing a chronoamperometry experiment at thin film's onset potential using a micro-GC 990 with an MS5A SS column. The injection time was 200 ms with an injector temperature of 90 °C and a column temperature of 145 °C at a pressure of 28 PSI. The analysis time was 60 s, with the gas cloud punctured every 30 min over a 3-h period.

3. Results and discussion

3.1. Photodegradation of the AO7: investigation of photocatalytic properties

Fig. 2 shows photodegradation results of AO7 for powder materials under xenon irradiation. The TiO_2-GC and TiO_2–CoN0.25-GC exhibit a comparable degradation rate of 38% after 7 h. This rate goes down with the material with the highest cobalt content, TiO_2–CoN0.5-GC, reaching 26%.

The enhanced visible absorption of TiO_2–Co_3O_4 hybrid materials, as demonstrated in our most recent publication, is attributed to the presence of cobalt [53]. Furthermore, the elevated specific surface area indicated in Table 1 suggests that these hybrid powders may demonstrate a superior degradation rate under xenon irradiation. But several variables independent on the materials can influence the photocatalytic degradation process, including the initial dye concentration, catalyst amount, pH, irradiating light source, and dissolved oxygen concentration [64,65]. One of the proposed hypotheses is that the pH of a solution affects the surface charge of thin films and then the adsorption of AO7. This influence is likely due to changes in the electrostatic effect between

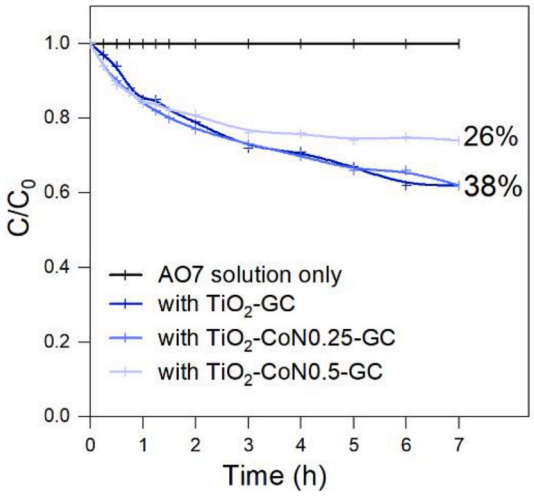

Fig. 2. Photodegradation curves of AO7 under xenon light for 7 h for the solution only (in black) and in presence of the three materials (in blue). (For interpretation of the references to color in this figure legend, the reader is referred to the Web version of this article.)

AO7 and the surface of the photocatalyst. As AO7 is an anionic dye by nature with a sulfonate function (pKa = 8.3 and 11.4), it will be negatively charged in an acidic solution and can be protonated in an alkaline solution, thereby becoming positively charged [66]. Therefore, under acidic conditions, electrostatic attraction could facilitate adsorption of AO7 on the positively charged surface. The surface of the TiO_2 is positively charged in an acidic solution (equation (6)) and becomes negatively charged in an alkaline solution (equation (7)), as illustrated by the following reactions:

$$TiOH + H^+ \rightarrow TiOH_2^+ \quad (6)$$

$$TiOH + OH^- \rightarrow TiO^- + H_2O \quad (7)$$

In this solution, TiO_2 then behaves as a Lewis acid, and AO7, an aromatic compound, acts as a Lewis base, as it readily donates π electrons to the vacant d orbital of TiO_2. This facilitates the adsorption of AO7 onto the surface of the TiO_2-GC thin film, which explains why its activity is superior to that of mixed thin films [31].

It is therefore conceivable that TiO_2 would have a higher oxidizing activity at acidic pH than the $Co(OH)_2$ as previously demonstrated present on the surface of TiO_2–Co_2O_3 thin films [53]. For the TiO_2–CoN0.25 thin film, the enhanced absorption of photons from the visible range may offset the aforementioned phenomenon. However, for TiO_2–CoN0.5-GC, which in principle has the largest number of $Co(OH)_2$ groups on its surface, this is no longer the case.

The impact of these findings on hydrogen production with a pollutant will be evaluated afterwards. The subsequent section will examine the impact of the pollutant presence on the electrochemical properties of these thin films.

3.2. Electrochemical impedance spectroscopy: effect of AO7 on electronic properties

Electrochemical impedance spectroscopy (EIS) in dark was studied as the optimal method for extracting resistances related to electronic charge transfer processes during the Oxygen Evolution Reaction (OER). To analyze Nyquist plots, which graphically represent the imaginary part of the impedance (Im Z, which is negative) as a function of the real part (Re Z) for a range of frequencies, we have defined an equivalent circuit that is suitable for our system. The circuit in question is depicted in Fig. 3 and is comprised of Rs, (Rp-1 CPE-1) and (Rp-2 CPE-2). Rs represents circuit elements such as electrical contacts and, above all, the electrolyte solution. Rp-1/CPE-p-1 corresponds to the ITO conductive substrate, while Rp-2/CPE-p-2 corresponds to the synthesized material thin film. CPE has been chosen instead of capacitance because it offered better fitting [67,68]. The objective here is not to compare thin films with one another, but rather to examine their electrochemical behavior in a model alkaline electrolyte or in a polluted alkaline electrolyte.

Fig. 4 shows Nyquist plots for the three thin films in both different electrolytes: model electrolyte (straight line), and polluted electrolyte (dot line). For all of them, two semicircles are observed, corresponding to the charge transfer resistances, Rp-1 and Rp-2. The high-frequency ordinate on the Re Z axis corresponds to the resistance Rs related to the electrolyte. The electrolyte conductivity is obviously affected by the presence of AO7, as the Rs value (Table 2) increases for all three thin films. The Rp-1 value is not discussed here because it is more related to the charge transfer at the interface between the film and the substrate, for which the influence of the pollutant is minor.

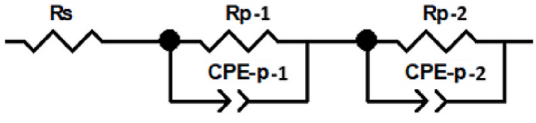

Fig. 3. Electric equivalent circuit of thin films.

Regarding the resistance Rp-2 corresponding to the thin film and representing the charge transfer between it and the electrolyte (Table 2), two distinct behaviors are observed in the polluted electrolyte. For TiO_2-GC and TiO_2–CoN0.25-GC samples, the presence of the pollutant notably reduces the Rp-2. This reduction is particularly pronounced in the case of the free cobalt layer. The presence of the pollutant in the solution for these two thin films is therefore not a limitation for the charge transfer mechanism, but rather an opportunity for improvement.

This result can be correlated with the adsorption phenomena discussed in the photodegradation investigation. During the electrochemical characterization process, the electrolyte is an alkaline solution with a pH value of 12. This indicates that the AO7 is in its protonated forms, which results in a net positive charge. As previously demonstrated, titanium dioxide is negatively charged in alkaline solution. This property enables TiO_2-GC to exhibit superior adsorption capacity for the AO7 molecule, thereby enhancing charge transfer at its interface with the electrolyte. This phenomenon is less apparent in TiO_2–CoN0.25-GC thin films, due to the surface presence of cobalt hydroxide. Nevertheless, it is present.

In contrast, the presence of the pollutant disrupts the charge transfer in the TiO_2–CoN0.5-GC layer due to a reduced adsorption capacity of the thin films, resulting in a slight increase in its Rp-2 resistivity. At the end, thanks to the high electronic conductivity of cobalt, this thin film still has the most effective charge transfer at the interface with the electrolyte, whether model or polluted.

3.3. Cyclic voltammetry under xenon light: impact of AO7 on the OER

To investigate the impact of AO7 on the OER, cyclic voltammetry was performed on the three samples (Fig. 5) in the model (straight line) and polluted (dot line) electrolytes under xenon irradiation. The voltammograms were evaluated from two perspectives: thermodynamically, by determining the onset potential (E_{onset}) through linear regression, which represents the beginning of the OER, and kinetically, by measuring the maximum current density (J_{max}). For all three thin films, it can be observed that the presence of the pollutant results in a delay in the onset of the OER. In fact, the value of the onset potential increases for all materials and in a relative manner with the presence of cobalt, for TiO_2-GC, +0.02 V; for TiO_2–CoN0.25-GC, +0.04 V and for TiO_2–CoN0.5-GC, +0.1 V. It appears reasonable to propose that the thermodynamic equilibrium may be disrupted because of the differing adsorption capacity of the layers.

About the kinetic aspect, both electronic and photocatalytic properties seem to control the photocurrent density. In the model electrolyte, it is evident that the good electronic conductivity of cobalt and the higher visible range absorption are beneficial to the OER rate, which is clearly visible in the current intensities recorded for mixed thin films, particularly for TiO_2–CoN0.5-GC with the highest cobalt content. The trend is less clear when it comes to the polluted electrolyte, due to the presence of AO7. The photocatalytic properties also control OER kinetics, as evidenced by the case of TiO_2–CoN0.25-GC, which presents intermediate charge transfer and photocatalytic properties. This thin film is the only one to display an increase in maximum current density in the presence of a polluted electrolyte, rising from 0.529 to 0.781 mA cm^{-2}. A noticeable decrease in the collected current is observed for the TiO_2-GC layer, with J_{max} dropping from 0.041 mA cm^{-2} in the model electrolyte to 0.003 mA cm^{-2} in the polluted electrolyte. The kinetics are also unfavorable for the TiO_2–CoN0.5-GC which loses about half of its maximum current (from 1.570 to 0.792 mA cm^{-2}).

In conclusion, it appears that the combination of optimal photocatalytic and electronic properties represents the most effective approach to achieving adequate electrochemical properties in polluted media. It remains to be seen whether a similar phenomenon will be observed in the case of hydrogen production, as well as in the coupling of water splitting and water remediation.

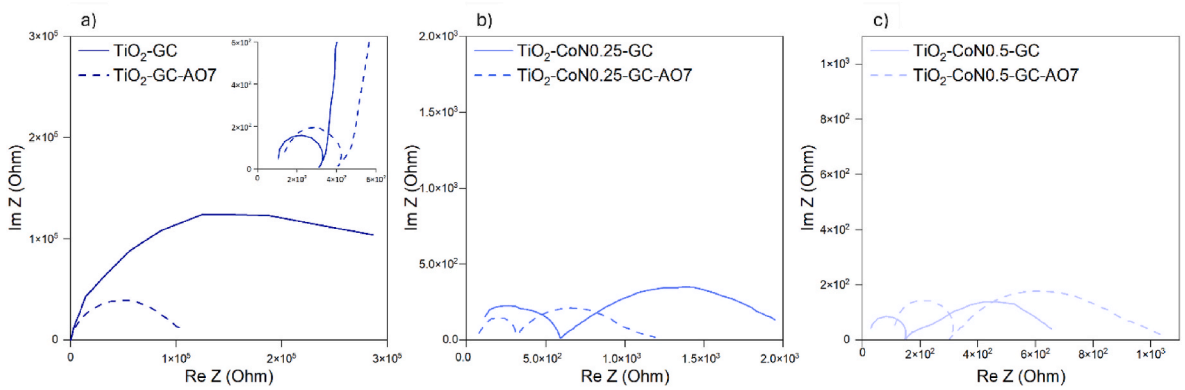

Fig. 4. Nyquist plots measured in dark in the model (straight line) and in the polluted (dot line) electrolyte for (a) TiO_2-GC, (b) TiO_2–CoN0.25-GC and (c) TiO_2–CoN0.5-GC thin films.

Table 2
Data derived from interpretation of Nyquist plots performed on thin films in the dark and from cyclic voltammetry under xenon light.

Parameters	TiO_2-GC		TiO_2–CoN0.25-GC		TiO_2–CoN0.5-GC	
	model electrolyte	polluted electrolyte	model electrolyte	polluted electrolyte	model electrolyte	polluted electrolyte
Rs (Ω)	118	163	70	104	33	128
Rp-2 (Ω)	306 771	98 243	954	563	332	396
E_{onset} *(V)*	1.84	1.86	1.62	1.66	1.62	1.72
J_{max} *(mA.cm^{-2})*	0.041	0.003	0.529	0.781	1.570	0.792

3.4. Hydrogen production and coupling of water splitting and water remediation

The production of hydrogen was investigated for thin films in model and polluted electrolytes during chronoamperometry measurements at E_{onset} +0.2 V for a period of 3 h under xenon light. The resulting production was plotted in Fig. 6.

No value could be presented for the TiO_2-GC layer in the polluted electrolyte, as the produced hydrogen quantity was below the device's detection limit. Equivalent production was observed for the TiO_2-GC thin film in the model electrolyte and for the TiO_2–CoN0.25-GC thin film in both electrolytes, between 1.2 and 1.8 μmol cm^{-2} h^{-1}. The TiO_2–CoN0.5-GC thin film, on the other hand, produced around 10 times more hydrogen in both electrolytes.

It is obvious that the presence of AO7 results in a reduction in hydrogen production for all thin films. This phenomenon can be attributed to a competition between hydrogen production and the photodegradation of AO7, which is influenced by the availability of electron/hole pairs. However, the TiO_2–CoN0.5-GC layer is the one that manages best to deal with the presence of the pollutant, despite its weak photocatalytic activity and negative impact on its photo-electrochemical properties. This indicates that optimal electronic conductivity is a requisite property of photo-electrochemical materials for attaining optimal performance.

To further elucidate the photocatalytic activity of the thin films in the PEC, we conducted a study on the photocatalysis and photo-electrocatalysis of AO7. The objective of this investigation was i) to ascertain the impact of sample form (powder or film) on photo-electrochemical properties and ii) to examine the influence of electronic contribution. Table 3 shows the AO7 photodegradation rate after 3h of photocatalysis and photo-electrocatalysis under xenon light for the thin films.

In the case of photocatalysis, the presence of cobalt clearly decreases the rate of photodegradation of AO7, as evidenced by the decreasing trend in photodegradation from 7.7 down to 3.9 % with increasing cobalt content. This negative effect of cobalt aligns with our previous findings concerning the photocatalysis investigation with powdered materials (part 3.1).

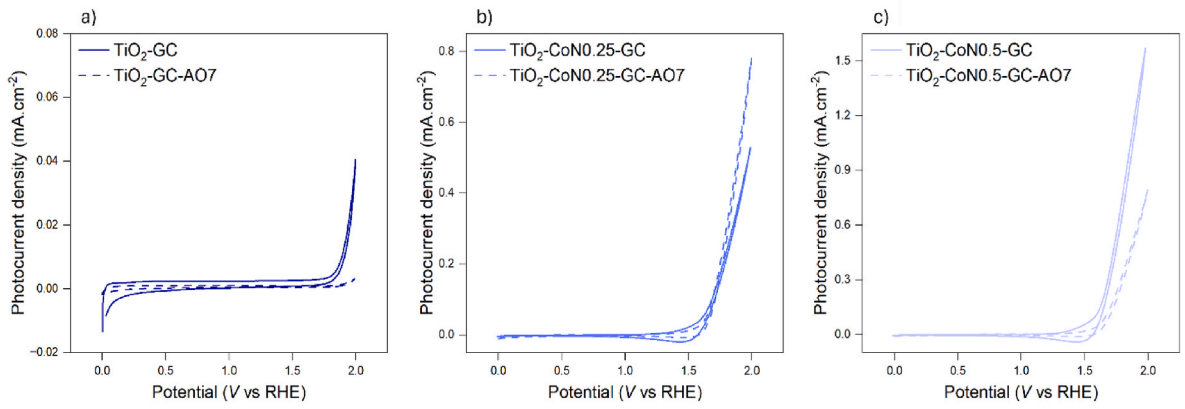

Fig. 5. Cyclic voltammetry in model (straight line) and polluted (dot line) electrolyte under xenon light for a) TiO_2-GC, b) TiO_2–CoN0.25-GC and c) TiO_2–CoN0.5-GC thin films.

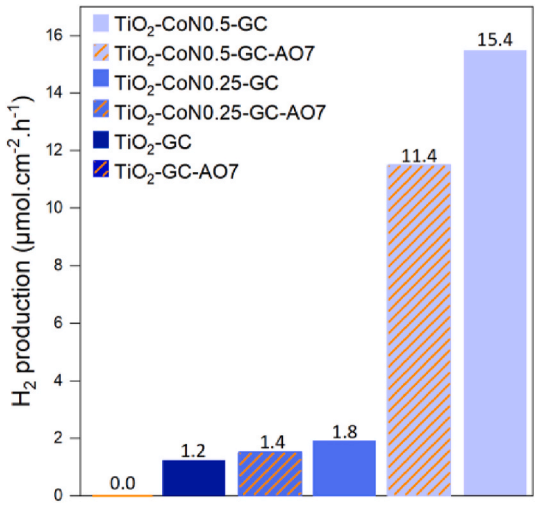

Fig. 6. Histogram of hydrogen production under xenon light using thin films.

Table 3
AO7 photodegradation percentage after 3 h under xenon light for the three thin films in the PEC.

Samples	Photodegradation percentage (%)	
	Photocatalysis	Photo-electrocatalysis
TiO_2-GC	*7.7*	*11.3*
*TiO_2–CoN0.*25-GC	*4.1*	*12.8*
*TiO_2–CoN0.*5-GC	*3.9*	*11.9*

Lastly, comparing photocatalysis and photo-electrocatalysis using thin films makes appear that the electric contribution is beneficial to the photodegradation of AO7 (11–13%), which proves that not only both hydrogen production and AO7 photodegradation can be envisaged simultaneously (as shown previously in Fig. 6), but more, that the electric contribution inherent to the hydrogen production can enhance the AO7 photodegradation [69,70].

Nevertheless, whatever the electric contribution may be concerned, the photocatalytic activity of thin films is much lower than that of powders. This can be due to several things, i.e. the amount of photocatalyst, the pH of the solution, the limited surface area for the adsorption of the AO7 on the thin films [66,71].

4. Conclusion

This article presents the continuation of our research on the synthesis of TiO_2–Co_3O_4-based hybrid materials as photoanodes for the production of hydrogen and the remediation of water. Following an investigation into the impact of bio-based surfactant and cobalt oxide presence on the morphological/structural and photo-electrochemical properties of synthesized TiO_2 thin films [52,53], the objective of this study was to examine the influence of a pollutant on the photo-electrochemical properties of three photoanodes with varying Ti/Co ratios.

The photocatalytic activity of these photoanodes in powder form was investigated through the photodegradation of AO7 under xenon light for a period of 7 h. It has been demonstrated that the pH of a solution can influences the surface charge of thin films and the adsorption of AO7 by modifying their electrostatic effect. An optimal adsorption of AO7 leads to an enhanced photocatalytic activity, a phenomenon previously observed in TiO_2-GC and TiO_2–CoN0.25-GC.

Furthermore, the EIS characterization demonstrates that a good adsorption property of the pollutant can also reduce the charge transfer resistance of the thin film in a polluted electrolyte, thereby improving the electronic conductivity properties. With regard to the photo-electrochemical properties, the outcomes of the cyclic voltammetry experiment indicated that the TiO_2–CoN0.25-GC thin film, which exhibited a synergistic combination of photocatalytic and electronic properties, demonstrated the greatest reactivity to the presence of the pollutant within the medium. Indeed, it was the only thin film to demonstrate an enhanced kinetic response during the OER, with a maximum current density rising from 0.529 to 0.781 mA cm^{-2}.

The final experiment of this study, which investigated the performance of the photoanodes by coupling hydrogen production and water remediation, yielded a different conclusion. It was observed that the TiO_2–CoN0.5-GC thin films exhibited the most optimal performance despite exhibiting the lowest photoactivity, with a production of hydrogen in the presence of a pollutant at a rate of 11.4 µmol cm^{-2} h^{-1} under xenon irradiation, accompanied by a simultaneous AO7 degradation of 12% without the use of a sacrificial agent. This suggests that the electronic conductivity of the photo-electrochemical material is a crucial factor in achieving optimal performance in PEC coupling for hydrogen production and wastewater treatment.

In the context of such experimental conditions and with a thin layer of TiO_2–Co_3O_4, the observed hydrogen production rate without the use of a sacrificial agent represents a previously unobserved phenomenon. These findings indicate that TiO_2–CoN0.5-GC thin films have the potential to be valuable materials for hydrogen production and pollutant degradation [27].

It would be beneficial to conduct a study with another real pollutant present in wastewater, such as a pharmaceutical compound, in order to gain further insights. The most far-reaching prospect would be the study of hydrogen production coupled with tertiary water purification treatment, using a real effluent from a wastewater treatment plant. In parallel with these approaches, the design of an "all-solid-state" photo-electrochemical cell for on-board applications, integrating photo-electrodes and a membrane electrolyte, is already under study.

CRediT authorship contribution statement

Fanny Duquet: Writing – review & editing, Writing – original draft, Visualization, Investigation, Formal analysis, Conceptualization. **Matthieu Rivallin:** Writing – review & editing, Validation, Supervision, Conceptualization. **Florence Rouessac:** Writing – review & editing, Validation, Supervision, Conceptualization. **Raphaël Costes:** Resources, Investigation. **Jim Cartier:** Resources, Formal analysis, Data curation. **Christophe Charmette:** Resources, Formal analysis, Data curation. **Stéphanie Roualdès:** Writing – review & editing, Validation, Supervision, Conceptualization.

Declaration of competing interest

The authors declare that they have no known competing financial interests or personal relationships that could have appeared to influence the work reported in this paper.

Acknowledgments

Thanks to Surfactgreen for providing the polymeric biosurfactant.

References

[1] Patz JA, Gibbs HK, Foley JA, Rogers JV, Smith KR. Climate change and global health: quantifying a growing ethical crisis. EcoHealth 2007;4:397–405. https://doi.org/10.1007/s10393-007-0141-1.
[2] Houghton J. Global warming. Reports Prog Phys 2005;68:1343–403. https://doi.org/10.1088/0034-4885/68/6/R02.
[3] Zandalinas SI, Fritschi FB, Mittler R. Global warming, climate change, and environmental pollution: recipe for a multifactorial stress combination disaster. Trends Plant Sci 2021;26:588–99. https://doi.org/10.1016/j.tplants.2021.02.011.
[4] Shen M, Huang W, Chen M, Song B, Zeng G, Zhang Y. (Micro)plastic crisis: unignorable contribution to global greenhouse gas emissions and climate change. J Clean Prod 2020;254:120138. https://doi.org/10.1016/j.jclepro.2020.120138.

[5] Yue M, Lambert H, Pahon E, Roche R, Jemei S, Hissel D. Hydrogen energy systems: a critical review of technologies, applications, trends and challenges. Renew Sustain Energy Rev 2021;146:111180. https://doi.org/10.1016/j.rser.2021.111180.

[6] Rosen MA, Koohi-Fayegh S. The prospects for hydrogen as an energy carrier: an overview of hydrogen energy and hydrogen energy systems. Energy, Ecol Environ 2016;1:10–29. https://doi.org/10.1007/s40974-016-0005-z.

[7] Parra D, Valverde L, Pino FJ, Patel MK. A review on the role, cost and value of hydrogen energy systems for deep decarbonisation. Renew Sustain Energy Rev 2019;101:279–94. https://doi.org/10.1016/j.rser.2018.11.010.

[8] Hore-Lacy I. Nuclear energy in the 21st century: the world nuclear university primer. 2011.

[9] Li Z, Fang S, Sun H, Chung R, Fang X, He J. Solar hydrogen. Adv Energy Mater 2023;13:1–26. https://doi.org/10.1002/aenm.202203019.

[10] Chapman A, Itaoka K, Farabi-Asl H, Fujii Y, Nakahara M. Societal penetration of hydrogen into the future energy system: impacts of policy, technology and carbon targets. Int J Hydrogen Energy 2020;45:3883–98. https://doi.org/10.1016/j.ijhydene.2019.12.112.

[11] Nnabuife SG, Ugbeh-Johnson J, Okeke NE, Ogbonnaya C. Present and projected developments in hydrogen production: a technological review. Carbon Capture Sci Technol 2022;3:100042. https://doi.org/10.1016/j.ccst.2022.100042.

[12] Cho HH, Strezov V, Evans TJ. A review on global warming potential, challenges and opportunities of renewable hydrogen production technologies. Sustain Mater Technol 2023;35:e00567. https://doi.org/10.1016/j.susmat.2023.e00567.

[13] Holkar CR, Jadhav AJ, Pinjari DV, Mahamuni NM, Pandit AB. A critical review on textile wastewater treatments: possible approaches. J Environ Manage 2016;182:351–66. https://doi.org/10.1016/j.jenvman.2016.07.090.

[14] Yaseen DA, Scholz M. Textile dye wastewater characteristics and constituents of synthetic effluents: a critical review, vol. 16. Springer Berlin Heidelberg; 2019. https://doi.org/10.1007/s13762-018-2130-z.

[15] Rafiq A, Ikram M, Ali S, Niaz F, Khan M, Khan Q, et al. Photocatalytic degradation of dyes using semiconductor photocatalysts to clean industrial water pollution. J Ind Eng Chem 2021;97:111–28. https://doi.org/10.1016/j.jiec.2021.02.017.

[16] Al-Mamun MR, Kader S, Islam MS, Khan MZH. Photocatalytic activity improvement and application of UV-TiO_2 photocatalysis in textile wastewater treatment: a review. J Environ Chem Eng 2019;7:103248. https://doi.org/10.1016/j.jece.2019.103248.

[17] Pinheiro HM, Touraud E, Thomas O. Aromatic amines from azo dye reduction: status review with emphasis on direct UV spectrophotometric detection in textile industry wastewaters. Dye Pigment 2004;61:121–39. https://doi.org/10.1016/j.dyepig.2003.10.009.

[18] Konstantinou IK, Albanis TA. TiO_2-assisted photocatalytic degradation of azo dyes in aqueous solution: kinetic and mechanistic investigations. Appl Catal B Environ 2004;49:1–14. https://doi.org/10.1016/j.apcatb.2003.11.010.

[19] Ardo S, Fernandez Rivas D, Modestino MA, Schulze Greiving V, Abdi FF, Alarcon Llado E, et al. Pathways to electrochemical solar-hydrogen technologies. Energy Environ Sci 2018;11:2768–83. https://doi.org/10.1039/C7EE03639F.

[20] Chiu Y-H, Lai T-H, Kuo M-Y, Hsieh P-Y, Hsu Y-J. Photoelectrochemical cells for solar hydrogen production: challenges and opportunities. Apl Mater 2019;7. https://doi.org/10.1063/1.5109785.

[21] Matsumoto H. Photoelectrochemical cells. Electrochem. Asp. Ion. Liq. 2011;414:221–34. https://doi.org/10.1002/9781118003350.ch15. Wiley.

[22] Fernandez-Ibanez P, McMichael S, Rioja Cabanillas A, Alkharabsheh S, Tolosana Moranchel A, Byrne JA. New trends on photoelectrocatalysis (PEC): nanomaterials, wastewater treatment and hydrogen generation. Curr Opin Chem Eng 2021;34:100725. https://doi.org/10.1016/j.coche.2021.100725.

[23] Walter MG, Warren EL, McKone JR, Boettcher SW, Mi Q, Santori EA, et al. Solar water splitting cells. Chem Rev 2010;110:6446–73. https://doi.org/10.1021/cr1002326.

[24] Rajput H, Kwon EE, Younis SA, Weon S, Jeon TH, Choi W, et al. Photoelectrocatalysis as a high-efficiency platform for pulping wastewater treatment and energy production. Chem Eng J 2021;412:128612. https://doi.org/10.1016/j.cej.2021.128612.

[25] Rauf MA, Ashraf SS. Fundamental principles and application of heterogeneous photocatalytic degradation of dyes in solution. Chem Eng J 2009;151:10–8. https://doi.org/10.1016/j.cej.2009.02.026.

[26] Clarizia L, Nadagouda MN, Dionysiou DD. Recent advances and challenges of photoelectrochemical cells for hydrogen production. Curr Opin Green Sustain Chem 2023;41:100825. https://doi.org/10.1016/j.cogsc.2023.100825.

[27] Pitchaimuthu S, Sridharan K, Nagarajan S, Ananthraj S, Robertson P, Kuehnel MF, et al. Solar hydrogen fuel generation from wastewater—beyond photoelectrochemical water splitting: a perspective. Energies 2022;15:7399. https://doi.org/10.3390/en15197399.

[28] Rioja-Cabanillas A, Valdesueiro D, Fernández-Ibáñez P, Byrne JA. Hydrogen from wastewater by photocatalytic and photoelectrochemical treatment. JPhys Energy 2021;3:012006. https://doi.org/10.1088/2515-7655/abceab.

[29] Joy J, Mathew J, George SC. Nanomaterials for photoelectrochemical water splitting – review. Int J Hydrogen Energy 2018;43:4804–17. https://doi.org/10.1016/j.ijhydene.2018.01.099.

[30] Christoforidis KC, Fornasiero P. Photocatalytic hydrogen production: a rift into the future energy supply. ChemCatChem 2017;9:1523–44. https://doi.org/10.1002/cctc.201601659.

[31] Rauf MA, Meetani MA, Hisaindee S. An overview on the photocatalytic degradation of azo dyes in the presence of TiO_2 doped with selective transition metals. Desalination 2011;276:13–27. https://doi.org/10.1016/j.desal.2011.03.071.

[32] Singh R, Dutta S. A review on H_2 production through photocatalytic reactions using TiO_2/TiO_2-assisted catalysts. Fuel 2018;220:607–20. https://doi.org/10.1016/j.fuel.2018.02.068.

[33] Sari Y, Gareso PL, Armynah B, Tahir D. A review of TiO_2 photocatalyst for organic degradation and sustainable hydrogen energy production. Int J Hydrogen Energy 2024;55:984–96. https://doi.org/10.1016/j.ijhydene.2023.11.126.

[34] Rafique M, Hajra S, Irshad M, Usman M, Imran M, Assiri MA, et al. Hydrogen production using TiO_2-based photocatalysts: a comprehensive review. ACS Omega 2023;8:25640–8. https://doi.org/10.1021/acsomega.3c00963.

[35] Ma H, Xiaohui Lu, Luo X, Sun D, Wang G, Fu Y. Constructing core-shell structured Co_3O_4–$MnWO_4$ composite photoelectrode with superior PEC water purification performance. Chemosphere 2024;354:141648. https://doi.org/10.1016/j.chemosphere.2024.141648.

[36] Pradhan D, Falletta E, Dash SK. Enhanced and rapid photocatalytic degradation of toxic dyes by cobalt oxide and modified cobalt oxide under solar light irradiation. Opt Mater 2023;135:113368. https://doi.org/10.1016/j.optmat.2022.113368.

[37] Xie F, Guo J-F, Wang H-T, Chang N. Enhancing visible light photocatalytic activity by transformation of Co^{3+}/Co^{2+} and formation of oxygen vacancies over rationally Co doped ZnO microspheres. Colloids Surfaces A Physicochem Eng Asp 2022;636:128157. https://doi.org/10.1016/j.colsurfa.2021.128157.

[38] Chen Y, Wang H, Wu M, Wang J, Fan M, Dong L, et al. Modulating interface internal electric field for efficient charge separation in Co_3O_4/M-TiO_2 p-n junction. Surface Interfac 2024;48:104226. https://doi.org/10.1016/j.surfin.2024.104226.

[39] Zhao F, Ma H. Application of Co_3O_4 in photoelectrocatalytic treatment of wastewater polluted with organic compounds: a review. Crystals 2023;13:634. https://doi.org/10.3390/cryst13040634.

[40] Ranjith R, Renganathan V, Chen SM, Selvan NS, Rajam PS. Green synthesis of reduced graphene oxide supported TiO_2/Co_3O_4 nanocomposite for photocatalytic degradation of methylene blue and crystal violet. Ceram Int 2019;45:12926–33. https://doi.org/10.1016/j.ceramint.2019.03.219.

[41] Noor S, Sajjad S, Leghari SAK, Flox C, Kallio T. Efficient electrochemical hydrogen evolution reaction and solar activity via bi-functional GO/Co_3O_4–TiO_2 nano hybrid structure. Int J Hydrogen Energy 2020;45:17410–21. https://doi.org/10.1016/j.ijhydene.2020.04.240.

[42] Zhao Wenjing, Wang Yuqiong, Wang Junfang, Wang Zs Zixuan, Li Zhenquan. Synthesis of TiO_2/Co_3O_4 core-shell nanowire array and study on photo electrochemical water splitting. Conf. Soc. Sci. Nat. Sci. 2020. https://doi.org/10.38007/Proceedings.0001350.

[43] Nurul S, Moridon F, Anggraini D, Arifin K, Minggu LJ, Kassim MB. Photocatalytic hydrogen generation from water by TiO_2/Co_3O_4 composite photocatalysis. Malaysian J Anal Sci 2022;26:581–8.

[44] Anggraini D, Wardani PK, Agustina M, Awaluddin A, Arifin K. TiO_2/Co_3O_4 composite as photoanode of photoelectrochemical water splitting. J Phys Conf Ser 2019;1351:012032. https://doi.org/10.1088/1742-6596/1351/1/012032.

[45] Hao Z, Tian X, Wang C, Yu B, Wang L, Gao Y, et al. Preparation of mesoporous TiO_2/Co_3O_4 nanosheets for efficient photocatalytic oxygen and hydrogen evolution. ACS Sustain Chem Eng 2023;11:13709–17. https://doi.org/10.1021/acssuschemeng.3c03561.

[46] Xiao G, Pan J, Fu Y, Li C. Metal-Organic-Frameworks-driven hollow core-shell Co_3O_4/TiO_2 heterojunction for enhancement of photocatalytic hydrogen generation. J Phys Conf Ser 2021;2011:012089. https://doi.org/10.1088/1742-6596/2011/1/012089.

[47] Liu J, Ke J, Li Y, Liu B, Wang L, Xiao H, et al. Co_3O_4 quantum dots/TiO_2 nanobelt hybrids for highly efficient photocatalytic overall water splitting. Appl Catal B Environ 2018;236:396–403. https://doi.org/10.1016/j.apcatb.2018.05.042.

[48] Gadge SS, Chauhan R, Late DJ, Chaudhary IJ, Ashokkumar M, Gosavi S. Enhanced sunlight-driven catalysis for hydrogen generation and dye remediation using synergistic p-Co_3O_4/n-TiO_2 nanocomposites. Nanoscale Adv 2024;6:1661–77. https://doi.org/10.1039/D3NA01167D.

[49] Saeed M, Usman M, Ibrahim M, Haq A ul, Khan I, Ijaz H, et al. Enhanced photo catalytic degradation of methyl orange using p–n Co_3O_4-TiO_2 hetero-junction as catalyst. Int J Chem React Eng 2020;18. https://doi.org/10.1515/ijcre-2020-0004.

[50] Rashtbari S, Dehghan G, Marefat A, Khataee S, Khataee A. Proficient sonophotocatalytic degradation of organic pollutants using Co_3O_4/TiO_2 nanocomposite immobilized on zeolite: optimization, and artificial neural network modeling. Ultrason Sonochem 2024;102:106740. https://doi.org/10.1016/j.ultsonch.2023.106740.

[51] Yılmaz HÇ, Atalay FE, Kaya H, Erdemoğlu S. Sol–gel synthesis of TiO_2 on Co_3O_4-coated sporopollenin exine microcapsules (SECs) and photocatalytic performance of new semiconductor heterojunction material. Environ Sci Pollut Res 2022;29:78620–36. https://doi.org/10.1007/s11356-022-21357-w.

[52] Duquet F, Nada AA, Rivallin M, Rouessac F, Villeneuve-Faure C, Roualdes S. Influence of bio-based surfactants on TiO_2 thin films as photoanodes for electro-photocatalysis. Catalysts 2021;11:1228. https://doi.org/10.3390/catal11101228.

[53] Duquet F, Flaud V, Villeneuve-Faure C, Rivallin M, Rouessac F, Roualdès S. Hybrid photoelectrocatalytic TiO_2-Co_3O_4/$Co(OH)_2$ materials prepared from bio-based surfactants for water splitting. Molecules 2023;28:7599. https://doi.org/10.3390/molecules28227599.

[54] Zulfiqar M, Chowdhury S, Omar AA, Siyal AA, Sufian S. Response surface methodology and artificial neural network for remediation of acid orange 7 using TiO_2-P25: optimization and modeling approach. Environ Sci Pollut Res 2020;27:34018–36. https://doi.org/10.1007/s11356-020-09674-4.

[55] Cho J, Denes FS, Timmons RB. Plasma processing approach to molecular surface tailoring of nanoparticles: improved photocatalytic activity of TiO_2. Chem Mater 2006;18:2989–96. https://doi.org/10.1021/cm060212g.

[56] Zhang X, Sun DD, Li G, Wang Y. Investigation of the roles of active oxygen species in photodegradation of azo dye AO7 in TiO_2 photocatalysis illuminated by microwave electrodeless lamp. J Photochem Photobiol Chem 2008;199:311–5. https://doi.org/10.1016/j.jphotochem.2008.06.009.
[57] Zulfiqar M, Chowdhury S, Samsudin MFR, Siyal AA, Omar AA, Ahmad T, et al. Effect of organic solvents on the growth of TiO_2 nanotubes: an insight into photocatalytic degradation and adsorption studies. J Water Process Eng 2020;37:101491. https://doi.org/10.1016/j.jwpe.2020.101491.
[58] Han F, Kambala VSR, Dharmarajan R, Liu Y, Naidu R. Photocatalytic degradation of azo dye acid orange 7 using different light sources over Fe^{3+}-doped TiO_2 nanocatalysts. Environ Technol Innov 2018;12:27–42. https://doi.org/10.1016/j.eti.2018.07.004.
[59] Muthirulan P, Devi CN, Sundaram MM. TiO_2 wrapped graphene as a high performance photocatalyst for acid orange 7 dye degradation under solar/UV light irradiations. Ceram Int 2014;40:5945–57. https://doi.org/10.1016/j.ceramint.2013.11.042.
[60] Jum'h I, Abu-Aleqa R, Jumah R, Tavares CJ, Telfah A. Efficiency of TiO_2/Fe_2NiO_4 nanocomposite in photocatalytic degradation of acid orange 7 (AO7) under UV irradiation. Water, Air, Soil Pollut 2023;234:18. https://doi.org/10.1007/s11270-022-05978-y.
[61] Stylidi M, Kondarides DI, Verykios XE. Mechanistic and kinetic study of solar-light induced photocatalytic degradation of Acid Orange 7 in aqueous TiO_2 suspensions. Int J Photoenergy 2003;5:59–67. https://doi.org/10.1155/S1110662X0300014X.
[62] Chung KT. Azo dyes and human health: a review. J Environ Sci Heal - Part C Environ Carcinog Ecotoxicol Rev 2016;34:233–61. https://doi.org/10.1080/10590501.2016.1236602.
[63] Pandey A, Singh P, Iyengar L. Bacterial decolorization and degradation of azo dyes. Int Biodeterior Biodegrad 2007;59:73–84. https://doi.org/10.1016/j.ibiod.2006.08.006.
[64] Akpan UG, Hameed BH. Parameters affecting the photocatalytic degradation of dyes using TiO_2-based photocatalysts: a review. J Hazard Mater 2009;170:520–9. https://doi.org/10.1016/j.jhazmat.2009.05.039.
[65] Isimjan TT, Rohani S, Ray AK. Photoelectrochemical water splitting for hydrogen generation on highly ordered TiO_2 nanotubes fabricated by using Ti as cathode. Int J Hydrogen Energy 2012;37:103–8. https://doi.org/10.1016/j.ijhydene.2011.04.167.
[66] Xu S, Ng J, Zhang X, Bai H, Sun DD. Adsorption and photocatalytic degradation of Acid Orange 7 over hydrothermally synthesized mesoporous TiO_2 nanotube. Colloids Surfaces A Physicochem Eng Asp 2011;379:169–75. https://doi.org/10.1016/j.colsurfa.2010.11.032.
[67] Amano F, Koga S. Electrochemical impedance spectroscopy of WO_3 photoanodes on different conductive substrates: the interfacial charge transport between semiconductor particles and Ti surface. J Electroanal Chem 2022;921:116685. https://doi.org/10.1016/j.jelechem.2022.116685.
[68] Wang S, Zhang J, Gharbi O, Vivier V, Gao M, Orazem ME. Electrochemical impedance spectroscopy. Nat Rev Methods Prim 2021;1:41. https://doi.org/10.1038/s43586-021-00039-w.
[69] Koo MS, Cho K, Yoon J, Choi W. Photoelectrochemical degradation of organic compounds coupled with molecular hydrogen generation using electrochromic TiO_2 nanotube arrays. Environ Sci Technol 2017;51:6590–8. https://doi.org/10.1021/acs.est.7b00774.
[70] Wang T, Lin C-A, Xu S, Wang C-F, Chen C-W, Dong C-D, et al. Toward concurrent organics removal and potential hydrogen production in wastewater treatment: photoelectrochemical decolorization of methylene blue over hematite electrode in the presence of Mn(II). Appl Catal B Environ 2019;244:140–9. https://doi.org/10.1016/j.apcatb.2018.11.048.
[71] Cheng H-H, Chen S-S, Yang S-Y, Liu H-M, Lin K-S. Sol-gel hydrothermal synthesis and visible light photocatalytic degradation performance of Fe/N codoped TiO_2 catalysts. Materials 2018;11:939. https://doi.org/10.3390/ma11060939.